Transactions, **SMiRT-26**
Berlin/Potsdam, Germany, July 10-15, 2022
Division 05

Water Hammer Induced by the Vapor Condensation during a postulated LOCA in the Pressure Suppression System of ITER Nuclear Fusion Reactor: Experimental and Numerical Analyses

Luca Berti [1], Alessio Pesetti [2], Michele Raucci[3], Roberta Lazzeri[4], Biswanath Sarkar[5] and Donato Aquaro[6]

[1] PhD student, Dep. Civil and Ind. Eng., University of Pisa, Pisa, Italy (luca.berti@phd.unipi.it)
[2] Dr, Department of Civil and Industrial Engineering, Pisa, Italy (alessio.pesetti@for.unipi.it)
[3] Mr., Dep. Civil and Ind. Eng., University of Pisa, Pisa, Italy (michele.raucci@unipi.it)
[4] Dr., Dep. Civil and Ind. Eng., University of Pisa, Pisa, Italy (roberta.lazzeri@unipi.it)
[5] Dr., Senior Advisor, Iter Organization, St Paul Lez Durance Cedex - France (Biswanath.sarkar@iter.org)
[6] Prof., Dep. Civil and Ind. Eng., University of Pisa, Pisa, Italy (donato.aquaro@unipi.it)

ABSTRACT

This paper deals with the qualification of the main safety systems of the nuclear fusion reactor ITER: the Vacuum Vessel Pressure Suppression System (VVPSS). This safety system manages the Loss of Coolant Accident (LOCA) that could occur in the Vacuum Vessel (VV) in order to avoid that a significant increase of the internal pressure could breach the primary confinement barrier. Steam condensation occurs at sub-atmospheric pressure. This condition is original respect the usual applications of steam direct condensation in nuclear fission reactors. An extensive experimental research program, funded by ITER Organization, on reduced scale experimental rigs (scale 1/22 and 1/10) have been carried out at the University of Pisa.

Unstable condensation regimens occurred during some tests originating high intensity vibrations of the whole experimental rig. These events can be classified as Condensation Induced Water Hammer.
Pressure impulses and occurrence frequencies of CIWH have been estimated elaborating the acceleration signals and implementing numerical models of the sparger. The preliminary conclusion is that the condensation at sub atmospheric pressure and the present geometry of the sparger determine a larger band of CIWH occurrence frequency than similar phenomena at atmospheric pressure. A positive achievement is that steam condensation occurs also at very small values of sub-cooling.

INTRODUCTION

The International Tokamak Experimental Reactor (ITER) foresees a Steam Pressure Suppression System, which operates at sub atmospheric pressure, for mitigating Loss of Coolant Accidents. The Vacuum Vessel Pressure Suppression System (VVPSS) is made of four tanks 100 m^3 of volume each, partially filled by water (60%). The steam is injected in the water pool by means of spargers having 1000 holes.

A Large Scale Experimental Facility (LSEF) has been built at the University of Pisa, funded by ITER, for analysing the direct contact steam condensation at sub atmospheric pressure. The maximum steam mass flow rate corresponds to a 1/10 reduced scale while the geometrical scale is close to a full scale (1/1.09). In the 92 m^3 condensation tank, reduced scale or full scale spargers can be tested.
During some experimental tests with full scale sparger and 0.5 kg/s of steam, instable condensation regimes occurred which caused strong vibrations of the experimental set up and of the close buildings. The Chugging and the Condensation Induced Water Hammer (CIWH) inside the sparger could be the causes of this dangerous phenomenon.

Chugging regimen occurs at small steam mass flow rate and is characterized by intermittent steam-water flux from the sparger holes. The CIWH derives from a steam slug which is quickly condensed by subcooled liquid which surrounds it. The liquid, driven by the pressure difference, accelerates to fill the void left by the condensed steam. The kinetic energy acquired by the liquid is converted to a local pressure rise which is transmitted as pressure waves at the sound velocity. The pressure waves could lead dangerous loading conditions on the structural components.

CIWH has been experimentally and numerically studied by several scientists. Janez Gale et al. (2004) state that CIWH is a stochastic phenomenon. In fact, several tests demonstrated that for equal boundary conditions and equal initial conditions, the steam slug formation and the subsequent fast condensation produce different effects. Urban et al. (2014) found that the highest occurrence probability and the highest pressure load occur at a Froude number 0.6 with a degree of sub-cooling of $\Delta T = 60\ K$. They estimated the pressure peaks by three approaches: a) an analytical models based on the Jukowsky formulas, used for water hammer in monophasic flux; b) using RELAP 5 code; c) implementing 3D CFD codes.

Wan et al. (2018) investigated experimentally the CIWH in a horizontal pipe and determined two types of CIWH as function of steam mass flow rates and of sub-cooling temperatures: periodic and non-periodic. At low sub-cooling and high steam mass flux non-periodic CIWH occurs at frequencies ranging between 0.22 and 1.11 Hz. The stochastic nature of the non-periodic CIWH does not permit to develop a correlation for determining the frequency. Instead for periodic CIWH, Wan determined a dimensionless correlation for the Strouhal (S_t) number (proportional to the frequency) versus Jacob (Ja) and Froude (Fr) number:

$$S_t = 0.2005(Ja)^{1.0921}(Fr)^{-1.0616} \quad (1)$$

being $S_t = \frac{f D_i \rho_l}{u_0 \rho_s}$, the Strouhal number, $J_a = \frac{\rho_l C_{pl} \Delta T}{\rho_s h_{fg}}$ the Jacob number, Fr=$\frac{u_0}{\sqrt{g D_i}}$ the Froude number.

Chong et al. (2021) developed a different correlation to calculate the Strouhal number for periodic CIWH considering the aspect ratio (L/D) of the pipe:

$$S_t = 7.09(Ja)^{0.91}(Fr)^{-1.61}(\frac{L}{D})^{-0.83} \quad (2)$$

Gregu et al. (2016) defined, in the case of a vertical pipe, the Froude number as:

$$Fr = \frac{G/\rho_s}{\sqrt{g l_s}} \quad (3)$$

being *ls* the distance between the steam jet and the free water surface, G the steam mass flow rate per unit of area and ρ_s the steam density.

They analysed the CIWH for Froude numbers ranging between 10 and 38 and determined that the highest frequency of pressure peaks occurred for low Froude number and low water temperature (21-41 °C).

LARGE SCALE EXPERIMENTAL FACILITY FOR THE QUALIFICATION OF THE VACUUM VESSEL PRESSURE SUPPRESSION SYSTEM

A Large Scale Experimental Facility (LSEF) has been built at the University of Pisa for qualifying the Vacuum Vessel Pressure Suppression system (VVPSS) of ITER in the relevant accidental scenarios (Aquaro (2021), Pesetti (2021)). The main components of LSEF are: a condensation tank (ETT, 92 m^3), an electric Superheated Steam Generator (SSG, 1.8 Mw), two tanks (10 m^3 of volume each) filled of high pressure high temperature water, an auxiliary tank (15 m3) for reaching steady state conditions, a vacuum pump and steam mass flow rate control lines (Figure 1).

The condensation tank (ETT), 60% filled with softened water, is 8 m height and has an inner diameter of 4 m. Two spargers have been used: a reduced scale sparger with 100 holes (sparger A) and a full scale sparger B with 1000 holes (Figure 2). The 10 mm of diameter holes in both the spargers are distributed on 20 rows, occupying an area 266 mm height. Sparger B is made of a DN450 pipe of 14 mm of thickness. The sub-atmospheric conditions in the ETT are obtained by means a vacuum pump. The condensation tank is instrumented by 50 temperature sensors and 16 pressure sensors located in the water pool and in the upper vacuum space. A one-axial accelerometer, mounted on the external surface of the sparger, records accelerations in the steam jet direction. Strain gauges, located on the sparger supports,

measure forces and moments due to the steam condensation in the pool. Six video cameras, installed in the ETT, permit to record the images of the steam condensation regimes by different positions.

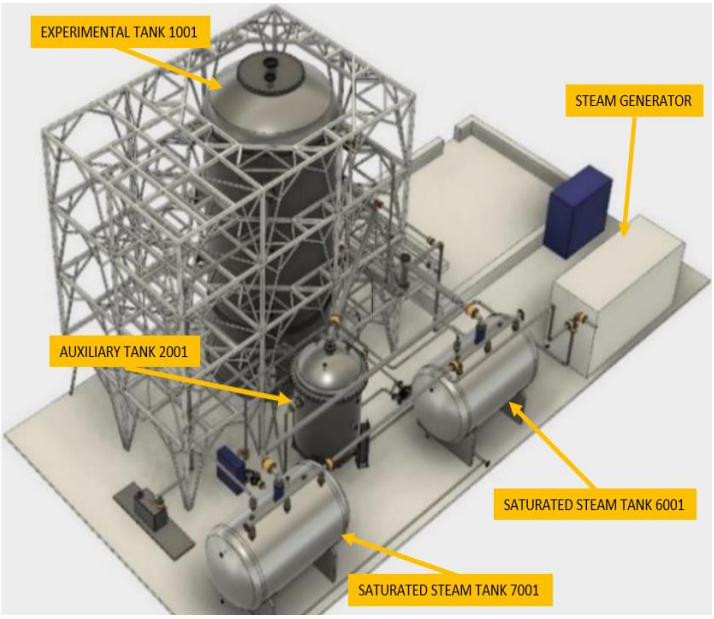

Figure 1: Layout of Full Scale Experimental Facility

Figure 2: sparger and accelerometer on the sparger support

EXPERIMENTAL TESTS

A test matrix of steam condensation with the sparger B and with a pool average temperature ranging between 16°C and 100°C has been performed in the Large Scale Experimental Facility. The steam mass flow rate ranges between 0-500 g/s, Pesetti (2021). The condensation regimes have been chugging or bubbling depending on the water temperature and the sub-cooling. Strong vibrations and CIWH occurred during some tests at constant steam mass flow rate (500 g/s).

Three condensation tests are examined in this paper corresponding at the following conditions:

- Water temperature in front of the sparger holes: 50°C, 60°C and 70°C;
- Sub-cooling in the water pool: 25°C, 18°C and 15°C, respectively;
- Steam mass flow rate: 500 g/s.

The duration of tests has been fixed in manner that the water average temperature increases of 2°C. Figure 3 illustrates the distribution of the temperature inside of the ETT in an instant of the three tests in exam. The temperature distribution is obtained by means of the elaboration of the temperature recorded inside the tank. A great stratification between the bottom and the holed zone of the sparger (temperature differences equal to 35°C, 40°C and 50°C, respectively) were recorded during all the tests.

In all three tests large accelerations of the sparger and pressure oscillations have been recorded. Figures 4-6 illustrate the acceleration signals for the three tests for a transient of 30 s. The large values of acceleration are associated at condensation phenomena classified ‘water hammer’. They occur mainly inside the sparger. Periodic chugging phenomena are visible (mainly in Figure 6-b) characterized by -0.1g÷-0.3g values of acceleration.

The pressure difference between the steam flux and the pool water (near the sparger holes) has an oscillatory trend and it reaches negative values for temperatures greater than Tw=50°C. This means that a

water reverse flow occurs during the test, that is, the steam flux is blocked and water of the pool enters in the sparger. Figures 7-9 illustrate the differences between the steam flux pressure (before entering in the sparger) and the pool water pressure in front of the sparger holes. In the same figures, the Power Spectral Densities (PSD) of these signals versus the frequency are shown. At Tw=50°C the pressure difference is almost always positive (average value equal to 2.5 kPa). The minimum value is a bit smaller than zero (-0.085 kPa). For greater temperatures, the average value is about 1 kPa and the minimum negative value is about half of the positive maximum value. In all the cases, the main peak of the PSD corresponds at frequencies ranging between 2.73Hz (T_w=50°C) and 2.29 Hz (T_w=70°C). These frequencies are associated at the intermittent steam flux from the sparger holes.

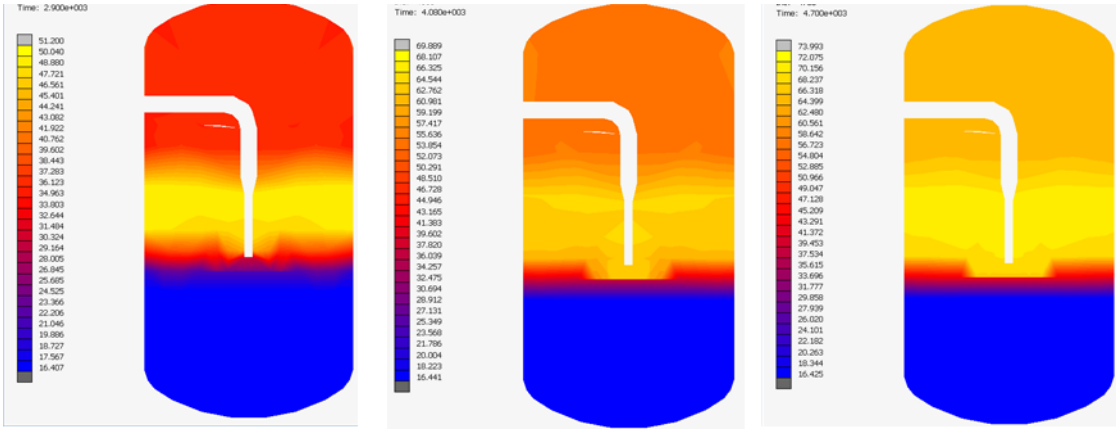

a) (test SST19) : Tw=50°C b) (test SST22)Tw=60°C c) (test SST23):Tw=70°C

Figure 3: Distribution of temperature in the ETT in the three tests in exam

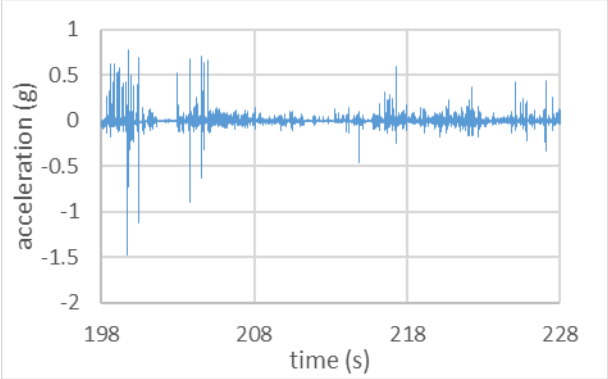

Figure 4 : Acceleration recorded in the test at Tw=50°C

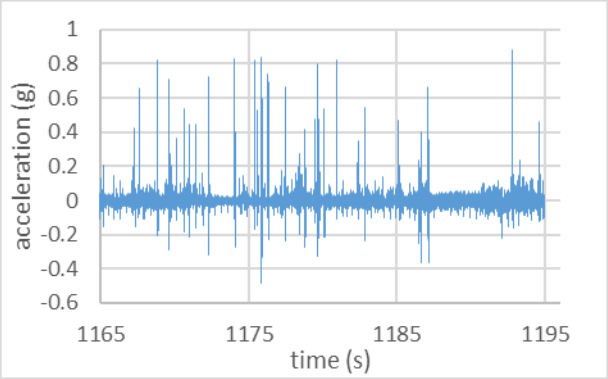

Figure 5 : Acceleration recorded in the test at Tw=60°C

Figures 10-12 show the steam jets exiting from the sparger at Tw=50°, 60° and 70°C, respectively. The frames have been obtained by video cameras (200 frame-rate per second), immerged in the condensation tank and located in front and down the sparger. At Tw=50°C (Figure 10) the steam exits always from the sparger holes even if some holes appear alternatively blocked. The time interval in which a same holed zone of the sparger comes back to be blocked is about 160-180 ms. It means to have cycles at 5-6 Hz. In fact, the PSD of the pressure difference between steam-water at Tw=50°C shows peaks in a large band of frequency ranging between 0.24 and 5 Hz (Figure 7).

The steam condensation images at Tw=60°C and 70°C (Figures 11-12) show that all the holes of the sparger are blocked in a particular instant of time. The cycle is repeated each 0.4-0.5 s, that is, with a frequency of

2-2.5 Hz. These values are confirmed by the PSD's (Figures 8-9) that show large peaks at 2.44 Hz (Tw=60°C) and 2.29 Hz (Tw=70°C).

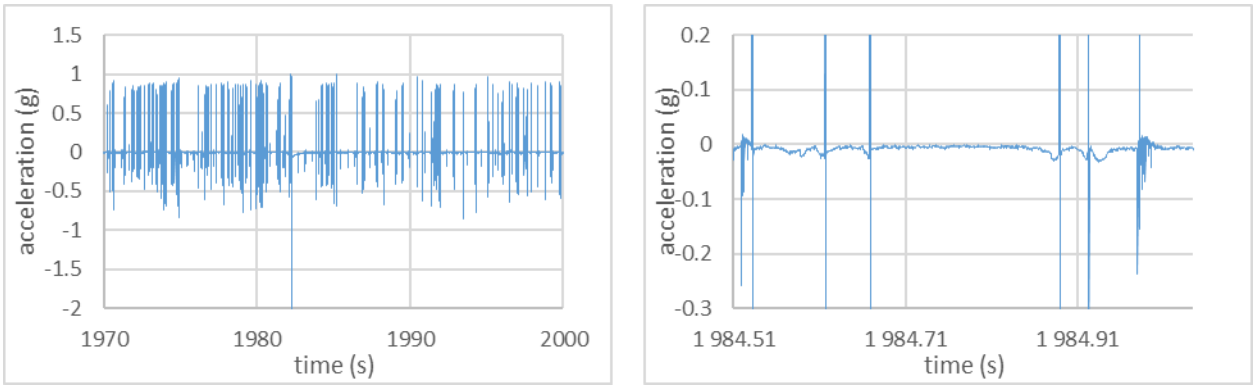

a) b)

Figure 6. Acceleration recorded in the test at Tw=70°C : a) 30 s transient (greatest peak equal to -5g) ; b) 0.5 s detail between negative peaks associated to the chugging

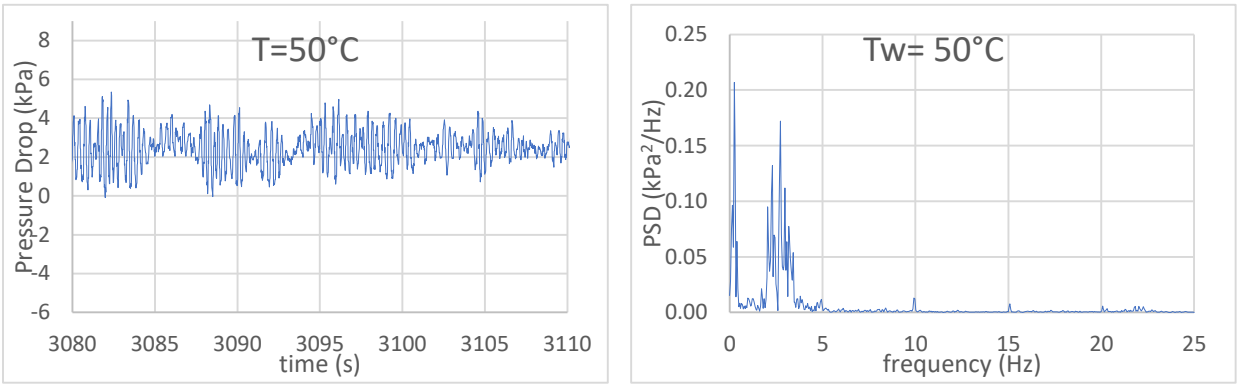

a) b)

Fig.7 Pressure difference between the steam flux (before entering in the sparger) and the pool water at Tw=50°C a); PSD versus frequency of the pressure difference signal (b)

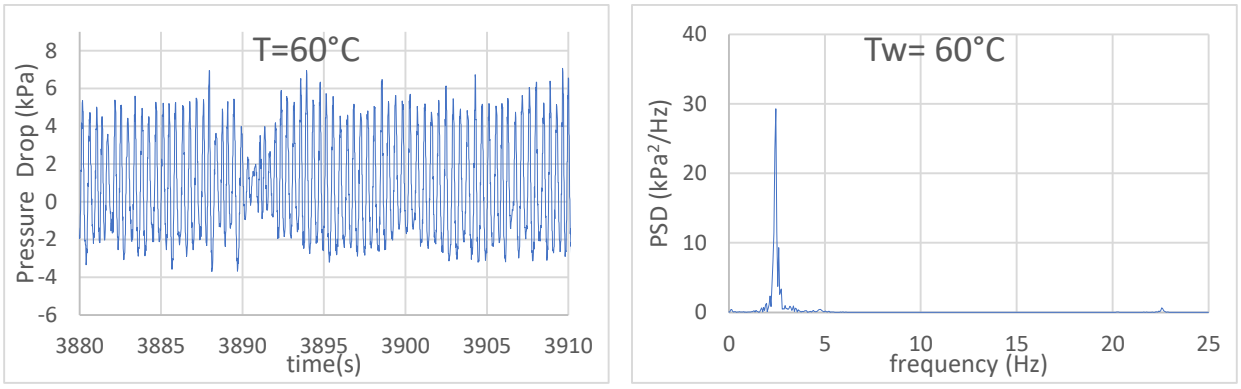

a) b)

Fig.8 Pressure difference between the steam flux (before entering in the sparger) and the pool water at Tw=60°C a); PSD versus frequency of the pressure difference signal (b)

These frequencies can be attributed at chugging in the water pool and can be associated at acceleration peaks having-0.1÷-0.3 g of value and distant each other 0.4-0.5 s (Figures 6 and 18). The water hammer

can be associated at -0.6 g÷+0.8g acceleration peaks having duration of about 20 ms (Figure 14). The acceleration signals show also few great negative peaks preceded by almost constant positive accelerations (Figure 17). The following paragraph describes numerical simulations which help to interpret the acceleration signals and permit to associate them a pressure peak or an impact force.

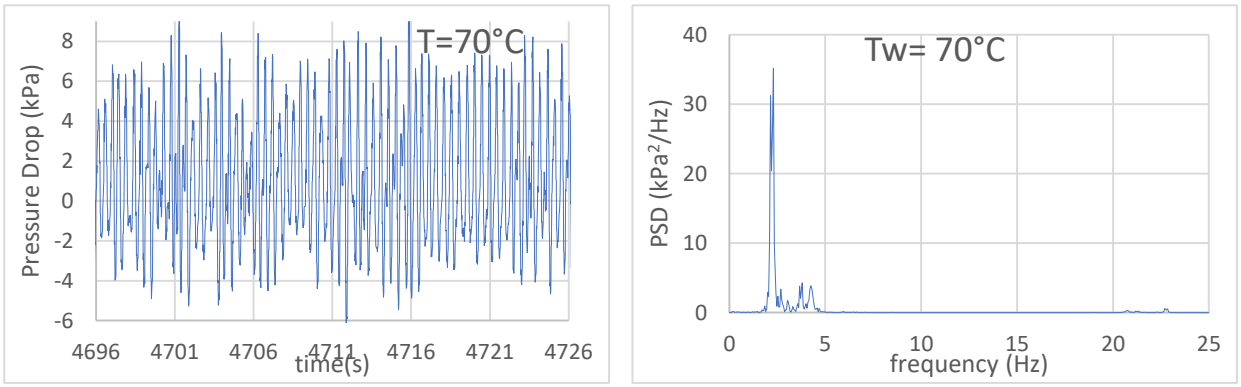

a) b)

Figure 9. Pressure difference between the steam flux (before entering in the sparger) and the pool water at Tw=70°C a); PSD versus frequency of the pressure difference signal (b)

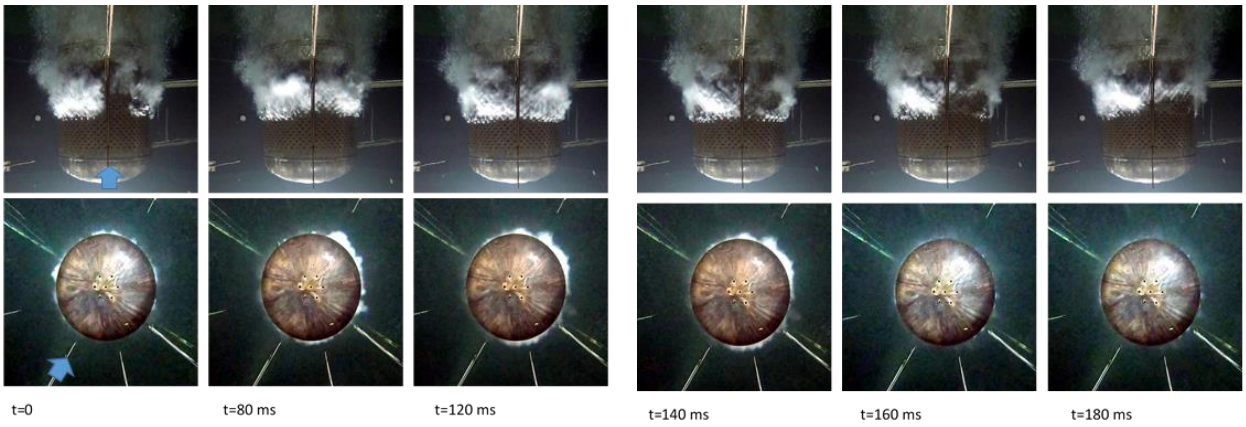

Figure 10 – frontal and bottom images recorded by the video cameras during the test corresponding a Tw=50°C

STRUCTURAL DYNAMIC BEHAVIOUR OF THE SPARGER: INTERPRETATION OF THE ACCELERATION SIGNALS BY MEANS OF NUMERICAL ANALYSES

The accelerometer is mounted on the external surface of a DN 300 schedule standard pipe and measures radial accelerations (Figure 2). This pipe supports the sparger and through it the steam flows towards the holed zone of the sparger. It can be analysed by means of a cylindrical shell model loaded by internal pressure as well as by a beam model supported vertically and horizontally by the tie rods. In the shell model, the radial displacements are proportional to the pressure load.

The pressure impulses, obtained integrating the acceleration signals, have been applied to an axial symmetric FEM model implemented using MSC-Marc computer code (Figure 13).

Figure 14 illustrates the comparison between numerical and experimental accelerations of the node corresponding to the position of the accelerometer. The very good agreement is obtained with a pressure impulse having a maximum value of 8.6 bar.

Results correspondent to another acceleration signal are depicted in Figure 15. In this case the maximum value of the pressure peak used in the numerical model is equal to 5.55 MPa.

Figures 16 shows an acceleration signal, characterized by a large almost constant positive acceleration followed by a greater negative peak. This shape cannot be associated to a pressure reverberation inside to pipe, but at a force parallel to the accelerometer axis which loads the pipe as a beam.

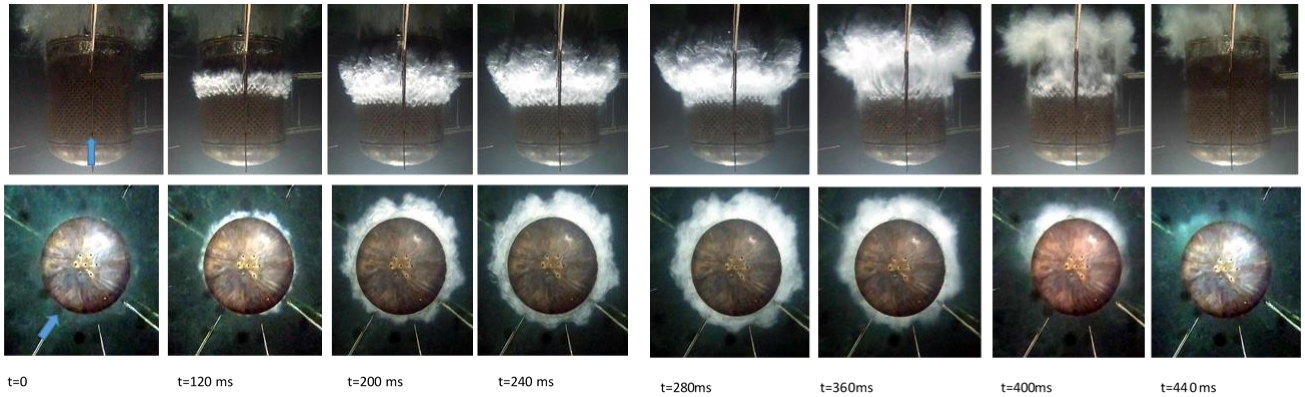

Figure 11 – frontal and bottom images recorded by the video cameras during the test corresponding a Tw=60°C

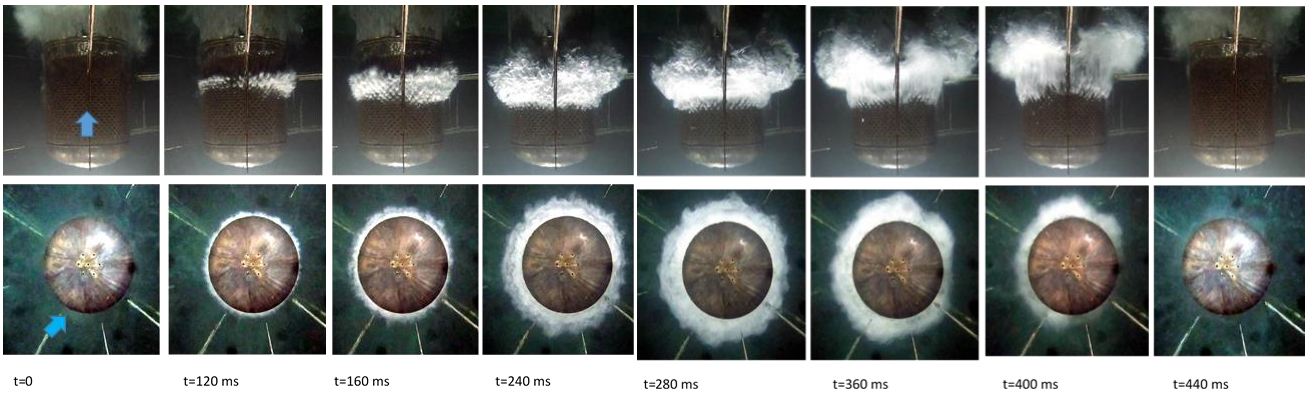

Figure 12– frontal and bottom images recorded by the video cameras during the test corresponding a Tw=70°C

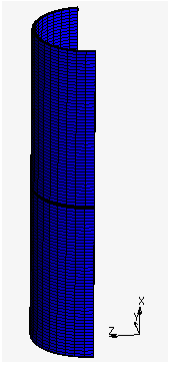

Figure 13. Mesh of the sparger support loaded by pressure impulse

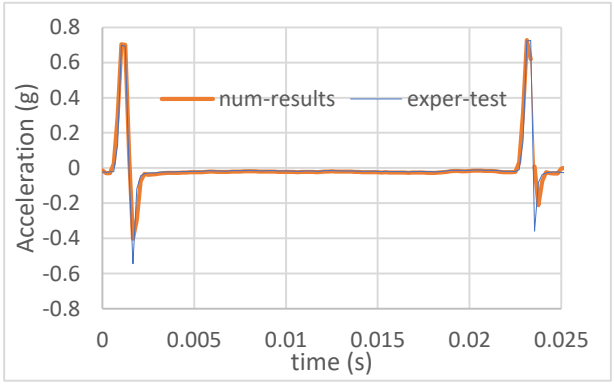

Figure 14. Comparison between numerical and experimental accelerations corresponding to a water hammer at Tw=70°C

A numerical model of the pipe as beam has been implemented applying a displacement history in correspondence of the accelerometer position. Figure 16 illustrates the displacement history and the comparison between the experimental and numerical accelerations. The maximum forces on the beam constraints are : 192 kN on the lower support (horizontal tie rods) and 95 kN on the upper support (the horizontal pipe).

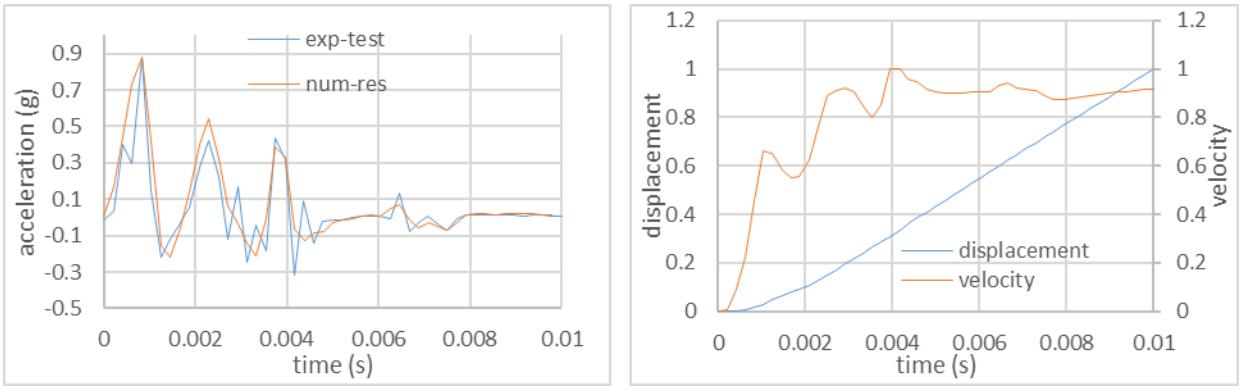

Figure 15 – Comparison of numerical and experimental accelerations associated at water hammers at 70°C (a) and corresponding normalized velocity and displacement (b) (maximum pressure impulse: 5.5 MPa)

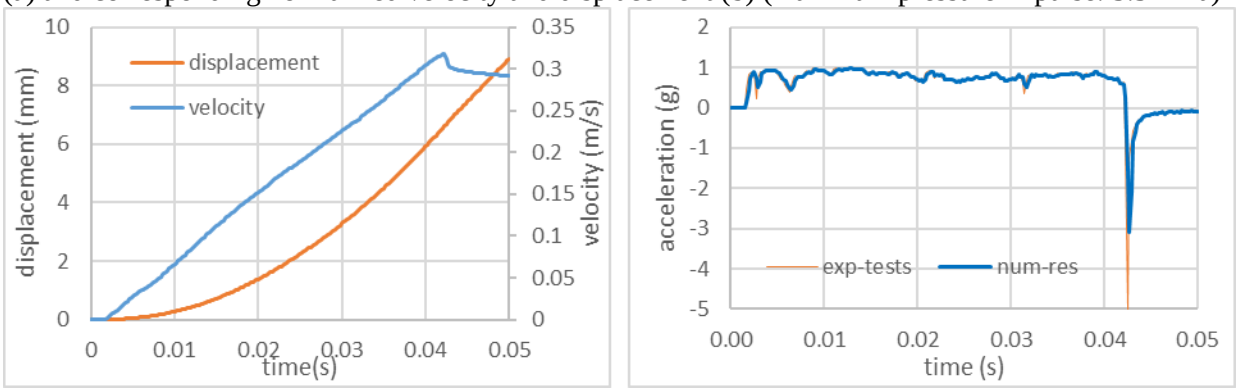

a) b)

Figure 16 - Velocity and displacement obtained integrating the acceleration signals a); Numerical and experimental accelerations associated at a water hammer at Tw=70°C b)

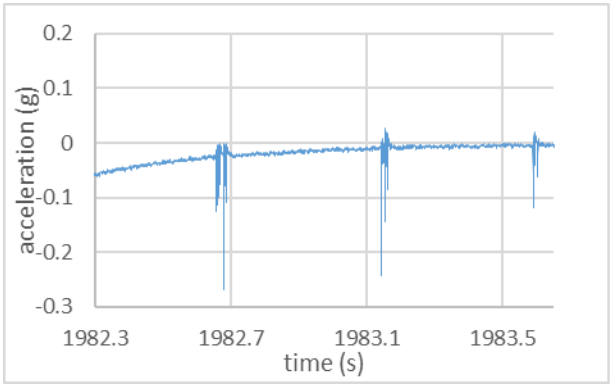

Figure 17. Accelerations peaks due to the chugging after a large negative peak corresponding to a water hammer

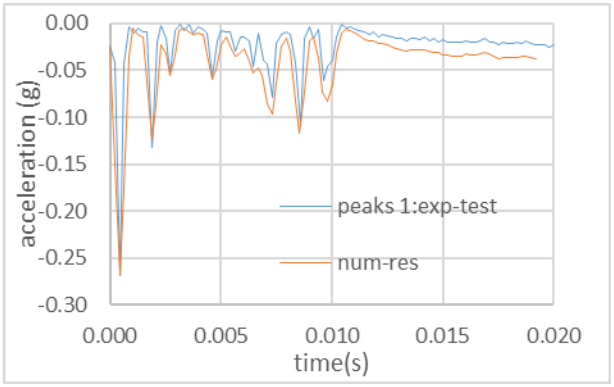

Figure 18. Numerical and experimental accelerations: chugging at 70°C (pressure impulse: 7.66 MPa)

The acceleration signals, shown in the Figures 14, 15 and 16, occur between negative acceleration peaks, associated at steam blockage during the chugging. These signals repeat themselves at T=70°C with a period of 0.4-0.5s (Figure 6). After an acceleration signal similar to that in Figure 16, these chugging signals occur without any other acceleration peaks between them. The three chugging signals, shown in Figure 17, have been elaborated with the shell model. The calculated maximum pressure impulses are:
Peaks 1: 7.66 MPa (Figure 18); Peaks 2: 4.14 MPa; Peaks 3: 2 MPa.

DISCUSSION OF THE RESULTS AND CONCLUSIONS

The geometry of the sparger determines two possible origin of the water hammer: the thermal hydraulic conditions inside the sparger and those of the pool water volume, surrounding the sparger.
During the tests in exam, a large thermal stratification occurred in the pool (Figure 3). Cold water at about 17°C has been aspirated inside the sparger through the holes located in the bottom, per effect of the depressurization determined by the steam collapse. The sub-cooling can have reached maximum values of 55-67°C in the three tests in exam.
Figure 19 depicts the occurrence frequency of the CIWH (in the three tests) determined with the empirical formulas proposed by Wan (2018) (equation1) in which the Froude number has been calculated using the expression for the vertical pipes reported in Gregu (2016) (equation 4).

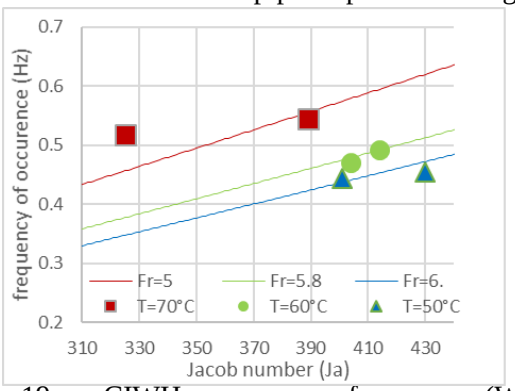

Fig. 19 – CIWH occurrence frequency (Wan (2018) modified equation).

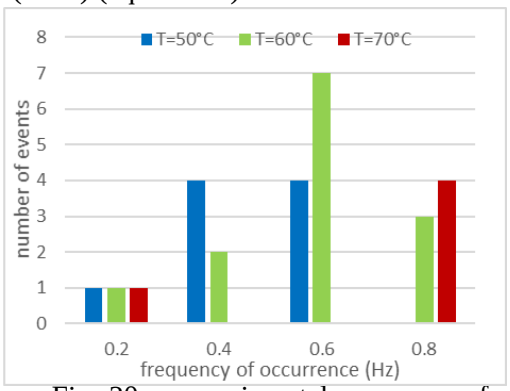

Fig. 20 – experimental occurrence frequencies at different water temperature

The thermal hydraulic conditions of the tests in exam correspond at Jacob and Froude numbers ranging in the following interval: $320 \leq Ja \leq 430$ $5 \leq Fr \leq 6$
The occurrence frequencies, determined by equation 1, are (Figure 19):

T_w=50°C: $0.44 \leq f\ (Hz) \leq 0.45$; T_w=60°C: $0.47 \leq f\ (Hz) \leq 0.49$; T_w=70°C: $0.51 \leq f\ (Hz) \leq 0.55$

The greatest experimental occurrence frequencies in the range 0÷1 Hz, determined by the elaboration of acceleration signals, are (Figure 20):
T_w=50°C : $0.4 \leq f\ (Hz) \leq 0.6$; T_w=60°C : $0.4 \leq f\ (Hz) \leq 0.8$; T_w=70°C : f= 0.8 Hz .
The theoretical estimation of frequencies, given by equation 1, fit sufficiently well the experimental results in this frequency range, despite the different test conditions.

The phenomena (chugging) which occur outside the sparger in the pool, illustrated by the Figures 10-12, are characterized by a reduced sub-cooling (14-20°C) and by greater occurrence frequencies. These chugging is a kind of water hammer, because the pool water blocks the steam flux. The occurrence frequencies can be described by a modified equation 1, considering the influence of the particular test conditions:

- The condensation potential expressed by the Jacob number must have a greater influence, because at sub-atmospheric pressure and in closed volume, steam condensation occurs also at very small sub-cooling;

- the kinetic energy of steam versus the potential energy of the water, expressed by the Froude number, has a minor effect considering the small value of steam pressure;

In this manner, a greater water mass flow rate than the steam mass flow rate, expressed by the Strouhal number, is obtained. A modified formulas could be the following:

$$S_t = (Ja)^{1.4}(Fr)^{-0.5} \quad (5)$$

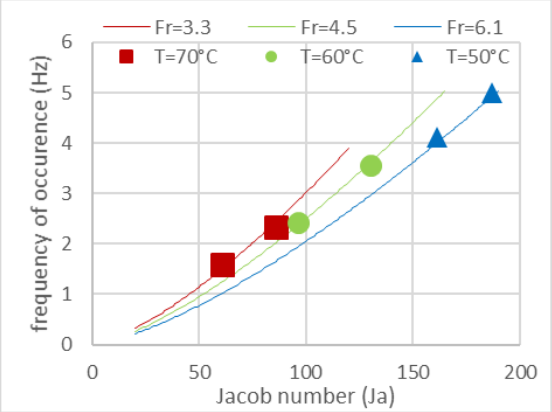

Fig. 21 – Chugging occurrence frequency

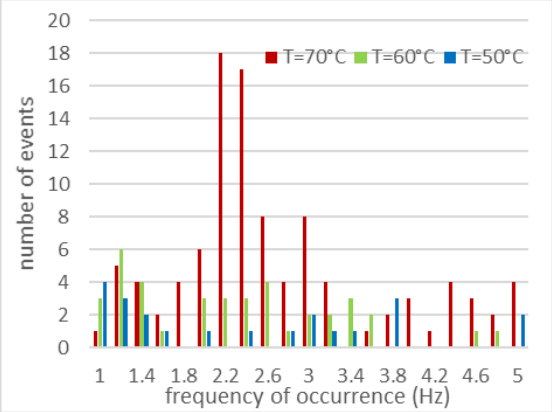

Fig. 22– experimental occurrence frequencies of chugging at different water temperature

Considering the thermal hydraulic conditions in the pool in front of the holed zone, the Jacob and Froude numbers range for the tests in exam in the following interval: 60≤ Ja ≤190 3.3≤ Fr ≤6.1

The occurrence frequencies, determined by equation 5, are (Figure 22):

T_w=50°C: 4.11≤ f (Hz)≤4.99; T_w=60°C: 2.4≤ f (Hz)≤3.5; T_w=70°C :1.6≤ f (Hz)≤2.34

Figures 22 shows the experimental values of the frequencies. The highest peaks (that is, the greatest number of events), correspond at the following frequencies:

- T_w=50°C: 1 Hz and 3.8 Hz; T_w=60°C: 1.2 Hz) and 3.4 Hz; T_w=70°C : 1.8 ≤ f (Hz)≤3 Hz

The previous values also agree with the frequencies of the pressure difference between the internal volume of the sparger and the pool, above all for the tests at T=60°C and T=70°C in which a total blockage of steam occurred. These results demonstrate that the CIWH could occur at sub atmospheric pressure in larger frequency band than in atmospheric direct condensation.

REFERENCES

Aquaro, D., et Alii *Experimental qualification of the ITER pressure suppression system by means of a large scale facility: Assessment of similitude analysis*,Nuclear Fusion, 2021, 61(12)

Chong, D., et Alii *Oscillation characteristics of periodic condensation induced water hammer with steam discharged through a horizontal pipe* Int. J. of Heat and Mass Transfer 173 (2021)

Gale J., et Alii, *Transition from Condensation-Induced Counter-Current Flow to Dispersed Flow*, Int. Conf. NENE 2004 - Portorož, Slovenia, Sept. 6-9, 2004

Gregu G., et alii , *Experimental Study on Steam Chugging Phenomenon in a Vertical Sparger*, Int. J. Multiphase Flow (2016)

Pesetti, A. et Alii *Large scale experimental facility for performance assessment of the vacuum vessel pressure suppression system of ITER* - Fusion Engineering and Design, 2021, 171,

Pesetti, A.,et Alii *Full scale test facility for operability verification of tokamak pressure suppression system at sub-atmospheric conditions* Fusion Engineering and Design, 2021, 168, 112639

Urban, C., et Alii *Investigations on stochastic nature of condensation induced water hammer* Int. J. Multiphase Flow 67 (2014) 1–9

Wang L., et Alii *Experimental investigation on the phenomenon of steam condensation induced water hammer in a horizontal pipe* Ex. Thermal and Fluid Science 91 (2018) 451–458